Diplomarbeit

Diagnostic value of ^{68}Ga-DOTA-NOC PET/CT in Somatostatin-receptor positive tumours of the gastrointestinal tract: a retrospective study

eingereicht von

Roman Ümit Safron

zur Erlangung des akademischen Grades

Doktor der gesamten Heilkunde

(Dr. med. univ.)

an der

Medizinischen Universität Graz

ausgeführt an der

Univ.-Klinik für Radiologie, Klinische Abteilung für Nuklearmedizin

unter der Anleitung von Dr.in med. univ. Tina Nazerani-Hooshmand

Univ. FÄ Dr.in med. univ. Susanne Stanzel

Univ.-Prof.in Dr.in med. univ. Reingard M. Aigner

Graz, am 14.11.2021

Eidesstattliche Erklärung

Ich erkläre ehrenwörtlich, dass ich die vorliegende Arbeit selbstständig und ohne fremde Hilfe verfasst habe, andere als die angegebenen Quellen nicht verwendet habe und die den benutzten Quellen wörtlich oder inhaltlich entnommenen Stellen als solche kenntlich gemacht habe.

Graz, am 14.11.2021 *Roman Ümit Safron eh*

Vorwort

Die Faszination für Physiologie, technische Innovation und der Wunsch, schwer kranken Patient*innen Hoffnung spenden zu können, waren ausschlaggebende Faktoren für die Durchführung und Entwicklung dieser Diplomarbeit. Die Forschung spielt eine wichtige Rolle in der evidenzbasierten Medizin, da Fortschritt und Innovation mit ihr ermöglicht werden. Die Suche nach der Wahrheit und die Ergründung neuer Horizonte sind jedoch schon so alt wie die Menschheit selbst. Diese Diplomarbeit stellte daher nicht nur eine sehr gute Gelegenheit dar, wichtige Werkzeuge für die Planung und Durchführung von Forschungsprojekten zu erlernen, sondern leistet auch einen Beitrag dazu, die Welt zumindest ein kleines Stück begreifbarer zu machen. Dafür bin ich sehr dankbar, und freue mich bei der Gestaltung einer Zukunft mitzuwirken, in der Einheit, Innovation und Hoffnung eine große Rolle spielen.

Danksagung

Besonders danke ich Frau.-Dr.in med. univ. Tina Nazerani-Hooshmand für ihre hervorragende Anleitung, Unterstützung und Vorbildwirkung.

Des Weiteren möchte ich Frau Univ.-Prof.in Dr.in med. univ. Reingard Aigner und Univ. FÄ Dr.in med. univ. Susanne Stanzel für die Ermöglichung und die Unterstützung an diesem Projekt danken.

Inhaltsverzeichnis

Inhalt

Glossar und Abkürzungen

AC- attenuation correction

AFP-Alpha Feto Protein

CD56-Cluster of Differentiation 56

CGA-Chromogranin A

CNS-Central Nervous System

G1/G2/G3-Grading 1/2/3

GEP-Gastroenteropancriatic

GI-Gastrointestinal tract

HCL-Hydrochloric Acid

5-HIAA-5-hydroxyindoleacetic

HPLC- High-Performance Liquid Chromatography

ITLC- Instant thin-layer chromatography

LOR-Line of Response

MBq-Megabecquerel

MRT- magnetic resonance imaging

NET-Neuroendocrine Tumour

NF1- neurofibromatosis type I

NSE-Neurospecific Enolase

SI-Small intestine

SPECT- Single-photon emission computed tomography

SRS-Somatostatin receptor scintigraphy

SSA-Somatostatin Analogs

SST-Somatostatin

SSTR- somatostatin receptor

TS- Tuberous sclerosis

WHO-World Health Organisation

Abbildungsverzeichnis

Tabellenverzeichnis

Zusammenfassung

Gegenstand: Das Ziel dieser retrospektiven Studie ist die Evaluierung der Bedeutung des ^{68}Ga-DOTA-NOC-PET/CT in der Diagnostik und im Grading von histologisch gesicherten neuroendokrinen Tumoren (NET) des Gastrointestinaltrakts (GI).

Methode: ^{68}Ga-DOTA-NOC-PET/CT-Untersuchungen von 31 Patient*innen mit histologisch gesichertem NET des GI wurden ausgewertet. Die Primärtumore des Magen-Darm-Trakts und deren Fernmetastasen, falls vorhanden, wurden mittels SUVmax- und SUVmean-Werten (maximum bzw. mean standardized uptake value) quantifiziert. Der SUVmax der Läsionen wurde mit der WHO-Klassifikation (G1, G2, G3) von NET- und Tumormarker-Werten verglichen. Bei der Analyse von SUVmax-Werten von Primär- und Sekundärtumoren wurden nur Patient*innen mit G1- und G2-Tumor berücksichtigt, da nur von einer Person Daten mit G3-Tumor vorlagen.

Ergebnisse: Mittels ^{68}Ga-DOTA-NOC-PET/CT konnten 26 Primärtumore im Colon ascendens, Colon descendens, im Bereich der Valvula ileocoecalis, des Coecums, Magens, Duodenums, Ileums und Jejunums bei 31 Patient*innen detektiert werden. Der SUVmax zeigte keine signifikante Korrelation mit G1- und G2-Tumoren. Signifikante Korrelation gab es zwischen dem Alter der Patient*innen und dem SUVmean. Weitere signifikante Korrelation gab es zwischen der Tumorlokalisation und dem SUVmax. Tumormarker zeigten keine signifikanten Korrelationen zu SUVmax-Werten.

Schlussfolgerung: ^{68}Ga -DOTA-NOC-PET/CT eignet sich als Werkzeug für das Staging von NETs des GI-Trakts. Es wird ermöglicht, Tumore in frühen Stadien zu entdecken. ^{68}Ga-DOTA-NOC-PET/CT ist der Diagnostik der Histopathologie unterlegen, da mit dem SUVmax-Wert G1 Läsionen nicht sicher von G2 Läsionen abgegrenzt werden können.

Abstract

Subject: The goal of this retrospective study is the evaluation of the value of ^{68}Ga-DOTA-NOC-PET/CT in diagnosing and staging of histologically verified neuroendocrine tumours (NET) of the gastrointestinal tract (GI).

Method: ^{68}Ga-DOTA-NOC-PET/CT images of 31 patients with histologically verified NET of the GI were analysed. Primary tumour sites of the GI-tract and the distant metastases, if present, were quantified via measurement of SUVmax- and SUVmean-values (maximum and mean standardized uptake value, respectively). The SUVmax of these lesions were compared with the WHO-classification(G1, G2, G3) of NET and tumour marker values. In the analysis of SUVmax-values with primary and secondary tumor sites, only patients with G1 and G2 tumours were considered, because only one patient with G3 tumour was present.

Results: Via ^{68}Ga-DOTA-NOC-PET/CT, 26 primary tumour sites in the colon ascendens, colon descendens, in proximity to the valvula ileocoecalis, caecum, stomach, duodenum, ileum, and jejunum amidst 31 patients could be detected. The SUVmax did not show significant correlation with G1 and G2 tumours. Significant correlation was present between age of patients and SUVmean. Another significant correlation was found between the tumour localisation and SUVmax-values. Tumour markers did not correlate significantly with SUVmax-values.

Conclusion: ^{68}Ga -DOTA-NOC-PET/CT is a suitable tool for staging of NETs of the GI-tract. It allows early detection of tumours in early stages. ^{68}Ga-DOTA-NOC-PET/CT is inferior to histopathological examinations because SUVmax-values do not differ between G1 and G2 lesions.

1 INTRODUCTION

1.1 Anatomy of duodenum and ileum

The duodenum and ileum, together with the jejunum, form the small intestine (SI). The SI absorbs high amounts of nutrients. To achieve high nutrient uptake, SI tissue forms layers that include a magnitude of small vessels, muscles and nerve cells. Four layers can be differentiated in the small intestine. Starting from the luminal side, the mucosa layer can be found. This layer's surface consists of villi, which improves the efficiency of absorption because a larger contact area is created. The villi structures consist of different specialised cells, including enteroendocrine cells. These enteroendocrine cells, particularly their malign proliferation, pose the subject-matter of our research. The submucosa follows the mucosa layer. It consists of connective tissue. In this tissue, blood and lymphatic vessels are embedded, combined with a network of nerve cells.

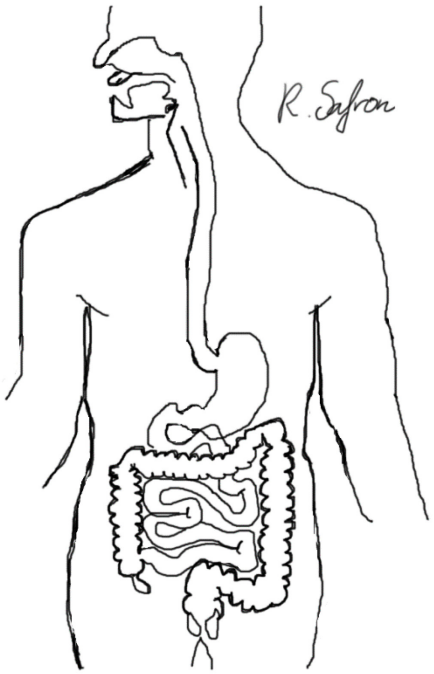

Figure 1: Schematic anatomical depiction of the gastrointestinal tract.

The third part is called the muscular layer. It consists of two layers of muscle cells, which embed nerve cells between them. The muscular layer is very important for the transportation of food in one direction.

The outer layer of the small intestine is called the serosa. Depending on the localisation, either mesothelial or epithelial cells are part of this tissue (1)

1.2 Physiology of duodenum and ileum

The small bowel absorbs four main types of nutrients; carbohydrates, proteins, fats, and vitamins.

Carbohydrates found in diets usually consist of polysaccharides. Enzymes like amylase break down the polysaccharides into smaller parts called monosaccharides. They are transported into the bloodstream using two different carriers, SGLT1 and GLUT5. These carriers can be found in the brush border of the small bowel.

The processing and absorption mechanism of proteins differs regarding the anatomical region of the gastrointestinal tract. In the stomach, pepsin and a low pH dissolve the peptide

bonds of proteins. The small bowel, however, uses a much higher pH and different enzymes derived from the pancreas.

Fats are usually found as triglycerides. Their breakdown begins lingual using enzymes. Further processing also occurs in the gaster using gastric lipases and in the duodenum using pancreatic enzymes. The physiological uptake of free fatty acids happens in the jejunum. Vitamins are absorbed in the small intestine. There are two types of vitamins, fat-soluble and non-fat soluble. Fat-soluble vitamins are A, D, E, and K. The jejunum and ileum are the most common sites for vitamin absorption.(2)

1.3 Neuroendocrine tumours

1.3.1 Types

Neuroendocrine cells are dispersed throughout the entire human body. They appear sporadically or accumulated in large groups. Endocrine cells secrete the largest amount of hormones, which gives them heterogenic characteristics, differing between the cell's localisation. Neuroendocrine tumours (NETs) are rare neoplasms of these cells. The gastrointestinal tract (GI) and the respiratory system are widespread places of origin for neuroendocrine tumours. Other entities also emerge from the pancreas, the central nervous system, and the skin. (3–5)

1.3.2 Incidence

The incidence of neuroendocrine tumours, especially of the gastroenteropancreatic (GEP) system, is steadily increasing. Neuroendocrine neoplasms usually develop in the upper intestine (stomach, esophagus) and pancreas. The colorectal region is also a common site for NETs. Neuroendocrine neoplasms of the gallbladder, liver, jejunum, and appendix are possible but uncommon. (6)

1.3.3 Staging

Grading of NETs is done by analysing their histopathological structure. These tumours are divided into two main groups: well-differentiated and poorly differentiated neuroendocrine tumours. Well-differentiated NETs are similar to physiological, endocrine tissue and form two main groups, Grade 1 (G1) and Grade 2 (G2). Poorly differentiated NETs are labeled Grade 3 (G3) neoplasms. They share very few similarities with physiological tissue, making them aggressive, rapidly progressing tumours. (7)

1.3.4 Ki67

Ki67 is a monoclonal antibody first manufactured in the city of Kiel (Ki). The number 67 refers to the first original clone of this antibody. Ki67 binds to proteins in the nucleolus, mostly present in G2 and M phases of the cell cycle. Under microscopic evaluation, Ki67 labeled, and unlabeled cells can be found. The difference between marked and unmarked nuclei shows the Ki67-idex. This index is quantified in percent. There are different cut-off values dependent on the tissue evaluated, which determines the tumour (G1, G2, G3). Ki67-Index has become an essential tool for grading of NETs. (8)

1.3.5 Genetics

Tumours with neuroendocrine properties often present themselves with different genetic findings. These findings can be associated with specific genetic syndromes or certain gene mutations.

Genetic syndromes often associated with neuroendocrine tumours are MEN-1, MEN-2 and a new MEN type called MEN IV. Moreover, Zollinger–Ellison syndrome, neurofibromatosis type I (NF1), Tuberous sclerosis (TS) and von Hippel–Lindau syndrome present themselves with gene mutations that pose a particular risk factor for the development of NETs. (9)

1.3.6 Signs and Symptoms

Neuroendocrine tumours of GI-tract are often asymptomatic or present themselves with indifferent abdominal pain. They are often accidental findings, which prolongs their diagnostic time. Jaundice and haemorrhage are uncommon but possible. (9) Excessive hormone secretion of NETs, although uncommon, can lead to the carcinoid syndrome. Presence of this syndrome raises the suspicion of hormone producing neoplasms. This differential diagnosis causes planning and initialisation of advanced blood tests and imaging modalities, oftentimes leading to lower diagnostic time. (4)

The carcinoid syndrome manifests in 3-13% of patients affected by GI-NETs. This state of highly elevated hormone secretion is challenging to control. Patients present a wide range of clinical manifestations, including flush, highly elevated bowel movements, respiratory problems, and stomach pain. This condition can only be treated symptomatically until the underlying cause is found.(10)

1.3.7 Prognosis

The prognosis of neuroendocrine tumours is based on two parameters, the Ki67-Index, and tumour grading. In SI-NETs, tumour size also plays a role in the prognosis concerning distant metastases. The 5-year survival rates for low-grade NETs of the midgut are at 79%.

Intermediate-grade neoplasms have a survival rate of 74%, and high-grade tumours show a survival rate of 40%.(11)

1.4 Tumour markers

Tumour markers can be tested in blood samples. Common tumour markers for detection of NETs are serotonin, chromogranin, and neuron-specific-enolase. Elevated tumour marker levels can indicate the presence of NETs. However, this is not enough to pinpoint the exact location of the tumour. (12)

Serotonin (5-hydroxytryptamine, 5-HT) is a hormone in the GI-tract that influences tissue function. Moreover, serotonin alters tumour growth. 5-HT tumour markers are commonly used to aid diagnosis and follow up of neuroendocrine neoplasms.(13)(14)

Chromogranin A (CgA) is a secretory protein. Endocrine and neuroendocrine cells secrete CgA into the blood to regulate blood vessel function. This biomarker is one of the best tumour markers to detect NETs. It is commonly used for follow-up evaluations of NETs.(15,16)

NSE (neuron-specific-enolase) detects the enolase produced by neurons and neuroendocrine cells. Elevated NSE levels can indicate an unusually high quantity of neuroendocrine cells in the body. This raises the suspicion that a NET is present. NSE is a useful tumour marker for GEP-NETs.(17)

1.5 Somatostatin

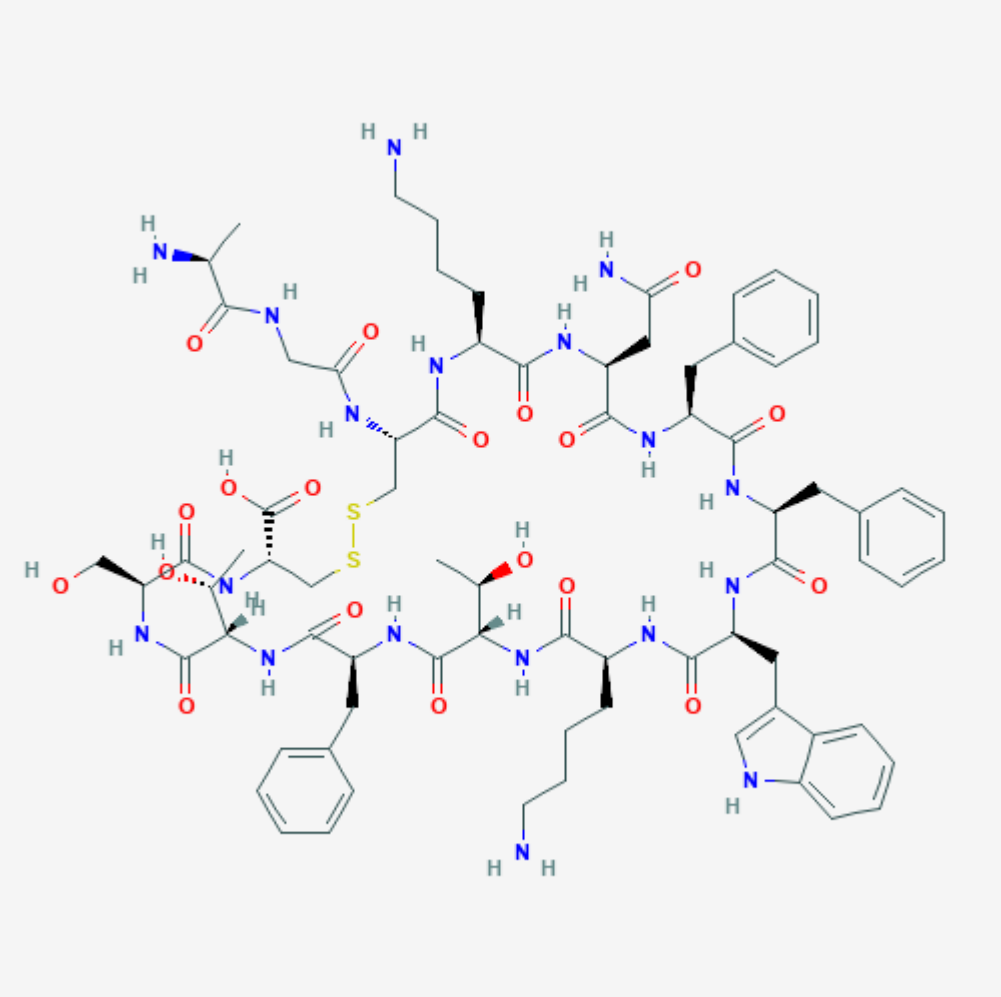

Figure 2: Chemical structure of non-synthetic somatostatin. It is a complex molecule with a short half-life. (18)

Somatostatin (SST) is a hormone that functions as a neurotransmitter. It has inhibitory properties and a very short half-life of just one to three minutes. SST suppresses both growth hormone and thyroid-stimulating hormone. It is mainly produced in the hypothalamus. SST is a cyclic tetradecapeptide. It consists of 14 to 25 amino acids and has a molecular weight between 11.5 to 15.7 kDa.(19)(20)

Somatostatin is mostly secreted in the central nervous system (CNS). Moreover, pancreas and GI also secrete this hormone. Other places of physiological secretion include the thyroid and lymphoid cells. SST can also be found in blood vessels and bloodstream. Last but not least, kidneys are also known sites of SST secretion. (20)

Somatostatin binds to five different receptor types, so-called somatostatin receptors (SSTR). These receptors are G-protein coupled. They can be located everywhere in healthy human tissue; however, the brain, pituitary gland, eyes, kidneys, pancreas, GI-tract, and heart are the most common physiological receptor accumulation sites. GEP-NETs mostly express

SSTR2 and SSTR5 receptor subtypes. This behaviour can be exploited for imaging and targeted therapy of GI-NETs.(19)

1.6 Therapy

Surgery is the primary treatment for neuroendocrine tumours. The tumour has to be correctly analysed prior to surgical procedures. Sometimes, other treatment modalities can be considered to aid surgery. Targeted therapy poses a different therapeutical approach, which can be used instead of surgery. However, surgical resection of NETs remains the only curative way.(21)

Targeted therapy of NETs is based on four main columns, hormone therapy, radioligand therapy (PRRT), chemotherapy, and surgery. Somatostatin analogs (SSA) build the foundation for treatment of well-differentiated neuroendocrine tumours. NETs express a high level of somatostatin receptors (SSTRs). SSAs bind to SSTRs. Consequently, SSAs modulate tumour growth and hormone secretion. However, extensive and prolonged use can lead to treatment resistance. (6)

Peptide-Radioreceptor Therapy (PRRT) is based on radionuclides, which are connected to somatostatin analogs. This substance binds to SSTRs and destroys the tumour with their radioactive payload. (22)

A new therapy modality is ^{177}Lu-DOTA-octreotate. It is a PRRT and shows promising results in treatment of neuroendocrine tumours. However, therapy response of neoplasms in the small intestine (SI-NET) is significantly lower compared to neuroendocrine tumours of the pancreas and rectum.(23)

1.7 Diagnosis

The diagnosis of a NET poses an essential step in oncologic management of patients. Most patients presenting NETs are between 50 to 60 years. Dependent on the suspected localisation of the neoplasm, different diagnostic modalities are available. First-line diagnostics include chest X-Rays and ultrasonography of the abdomen. Moreover, scans performed with Computed Tomography (CT) and magnetic resonance imaging (MRT) are a viable diagnostic option. For gastric and colorectal NETs, endoscopy is the choice. Furthermore, there are two particular modalities for NET diagnosis. One of them includes a group of diagnostic modalities called somatostatin receptor scintigraphy (SRS), performed with ^{111}In-pentetreotide (OctreoScan®). The second group includes new diagnostic methods with gallium labeled somatostatin analogs (SSAs), like PET/CT with ^{68}Ga-DOTA-NOC.(4,21)

1.8 ^{68}Ga-DOTA-NOC PET/CT

1.8.1 Characteristics of ^{68}Ga DOTA-NOC

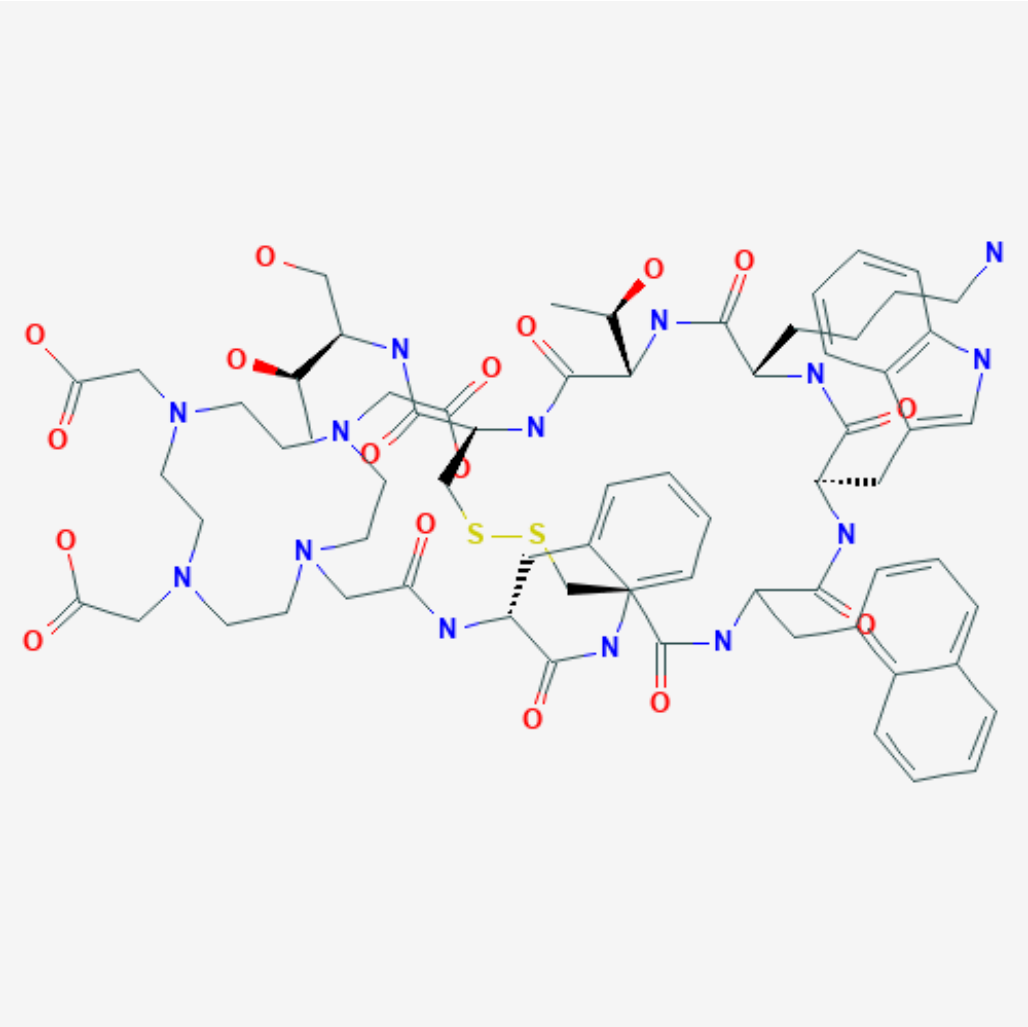

Figure 3: Structure of DOTA-NOC. The ^{68}Ga part of ^{68}Ga-DOTA-NOC is not depicted. In the end of the manufacturing process, ^{68}Ga is bound to the DOTA complex.(24)

1.8.2 Soamatostatin analogs

Native somatostatin (SST) has a very short half-life and therefore has only limited properties for clinical use. For this reason, synthetic analogues with longer half-lifes have been developed. Octreotide, Lanteroide, Vapreotide are SST analogues which are commonly used today. Their half-life lasts between 1.7 and 3.8 hours, which is significantly longer compared to native SSTs.(19)The DOTA-NOC complex of ^{68}Ga-DOTA is a modified version of Octreotide.(25)

^{68}Ga-DOTA-NOC is a radiopharmaceutical drug consisting of three parts. One is a peptide mimicking somatostatin. This peptide attaches specifically to SSTRs. (26)These receptors are scattered throughout the entire body. Physiological tracer uptake can be measured in the

pituary gland, salivary glands, spleen, liver, head of pancreas, and adrenal glands. The kidneys and bladder show high physiological uptake due to renal excretion of the tracer. (3)Physiological uptake of ^{68}Ga-DOTA-NOC can be detected in small lymph nodes and organs of the small pelvis, like the prostate and uterus. Moreover, breasts and the musculoskeletal system can show physiological uptake without indicating a NET. Sometimes, focal accumulations of ^{68}Ga-DOTA-NOC are present in lungs and brown fat. These physiological findings can lead to pitfalls in diagnosis of NETs and should be taken into consideration.(27)

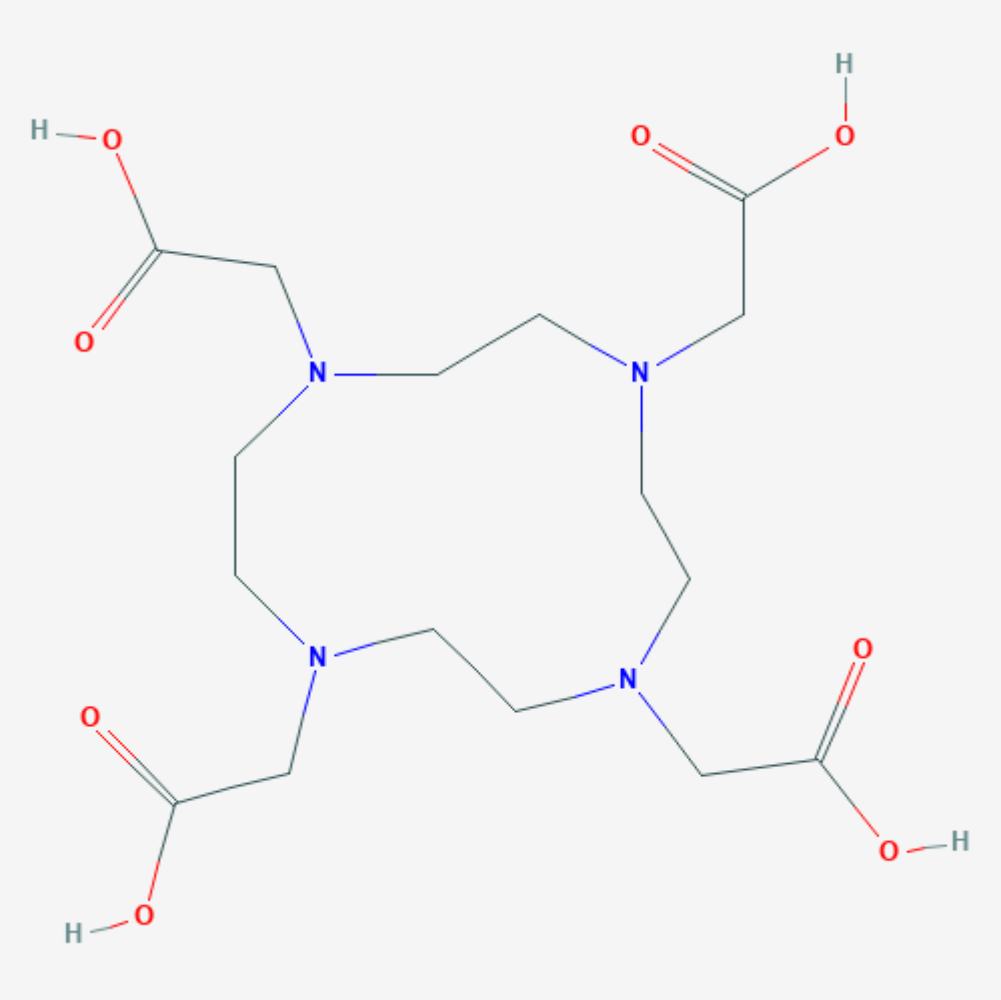

Figure 4: Structure of DOTA complex. This molecule serves as a connection between ^{68}Ga and the synthetic somatostatin analogue. (28)

The somatostatin analogue is connected to the DOTA complex, which is a chelator (Fig. 4). The third part consists of ^{68}Ga, which is a radionuclide eluted from the ^{68}Ge/^{68}Ga generator. It has a brief half-life of 68 minutes, which makes it well suited for clinical use. (29) ^{68}Ga binds to the chelator complex, which is the last step in the production of ^{68}Ga-DOTA-NOC. (26) This tracer is now ready for application and can be detected with a Positron Emission Tomography (PET) scanner. (3,26)

The PET scan is often coupled with a Computed Tomography (CT), which facilitates the determination of suspicious PET lesions with their anatomical location inside the body.

1.8.3 Synthesis of ^{68}Ga and labeling

^{68}Ga is eluted from a ^{68}Ge/^{68}Ga generator (Fig. 5). Modern ^{68}Ge/^{68}Ga generators are using a special silica resin, which is metal-free. This is an essential step to avoid contamination of ^{68}Ga with metal agents. Hydrochloric acid (HCL) is eluted through the generator and is carrying ^{68}Ga, which does not need to be purified and is ready for labelling with DOTA complexes. This method achieves high grades of both purity (>98%) and elution yields of approximately 80%.(30)

Labelling of ^{68}Ga with the DOTA-NOC complex is done in a glass vial. Both substances get mixed and heated up in a heating block. Temperatures in this unit are over 90 or over 121 degrees Celsius high. Samples that were heated up at around 90 degrees Celsius need to be filtrated through a 0.22 µm filter.(31)

Figure 5: Galli Ad® generator. Notice the green lead container on the right side; this is where the eluted ^{68}Ga is stored.

1.8.4 Quality control

Quality control of the final product can be assessed with many different tests. Testing of radiochemical purity is performed using chromatography. Two common methods are High-Performance Liquid Chromatography (HPLC) and Instant thin-layer chromatography (ITLC). Other important tests include sterility and absence of endotoxins in the product. Moreover, osmometry and pH tests are performed. (31)(25)

1.8.5 PET/CT TECHNOLOGY

Positron Emission Tomography (PET) is a device that consists of two key elements. One is the PET device itself, which is assembled of many crystals arranged in a circular pattern (Fig. 6). If one of these crystals gets hit by gamma rays, it produces a measurable signal.

The second key part is a radiopharmaceutical which is injected into the patient. This substance must be positron- emitting. The emitted positron collides with an electron and the annihilation effect takes place. This effect disperses two annihilation gamma rays in exactly opposite directions. For this reason, if two opposing crystals are hit at the same time, a line can be drawn between them. This line is known as Line of Response (LOR). With this data, the origin of the particles can be calculated.
However, the annihilation gamma rays can also collide with atoms of neighbouring tissues, which leads to random false positive, false negative or no LORs at all. Therefore, the acquired data must be corrected for different tissue effects. This correction is called attenuation correction (AC). In standalone PET devices, this correction was achieved with the use of an additional radioactive isotope located near to the crystal ring of the PET. This isotope moves along the ring and can provide data for AC. However, most modern PET devices are coupled with Computed Tomography (CT). Because CT uses circulating x-ray tubes, which emit radiation, data from the CT scan can be modified and used for AC. This achieves huge advantages, because the PET scan does not need an extra cycle for AC and is therefore shorter in duration. Furthermore, PET and CT scans can be computed together and provide fusion pictures, which allow for topographical and functional imaging. (32)(33)

The Standard Uptake Value (SUV) provides a semiquantitative analysis of radioactive activity in a specific area. AC is very important for measuring SUV accurately. (34) Recent findings show that the maximum SUV of NET can be used as a prognostic factor in conjunction with the differentiation of the tumour and presence of targeted therapy.(35)

Figure 6: PET/CT device. Patients undergoing examination are placed on the stretcher, which moves towards the ring depicted in the middle of the picture. First, they undergo a CT scan which is followed by a PET scan.

1.9 Other nuclear medicine examinations

Somatostatin receptor scintigraphy is a widespread method to detect NETs. This method uses synthetic somatostatin analogs which bind to different radionuclides, for example, ^{111}In and ^{99}Tc. These radionuclides are γ-emitter. The most common ones are ^{111}In-Octreotide and ^{99m}Tc-HYNIC-TOC. They are used in conjunction with gamma cameras, known as Single-photon emission computed tomography (SPECT), which can be extended with a CT-scan (SPECT-CT).(36)(37)(38)

^{111}In-Octreotide and ^{99}Tc-HYNIC-TOC are popular diagnostic methods for NET and GI-NET; however, PET/CT with ^{68}Ga labeled somatostatin analogs pose a better alternative. PET/CT with ^{68}Ga-DOTA-NOC and similar derivates show precise images of tumours. Faster decay of ^{68}Ga is beneficial because it provides a shorter evaluation time of 90 minutes in comparison to 24h in scans with ^{111}In-Octreotide SPECT. Moreover, PET/CT with somatostatin labeled ^{68}Ga-DOTA complexes detects more bowel NETs than 111In-Octreotide with a 96.1% sensitivity compared to 13.7%.(39)

^{99m}Tc-HYNIC-Octreotide SPECT scans of the GI-NETs showed a sensitivity of 50% compared to 100% in ^{68}Ga-DOTATATE PET/CT. ^{68}Ga-DOTATATE PET/CT also detects

significantly more lesions in the gastrointestinal tract compared to ^{99m}Tc-HYNIC-Octreotide SPECT. (40)

1.10 Other modalities

1.10.1 Computed Tomography

The computed tomography (CT) is a diagnostic tool that uses rotating X-ray tubes and detectors. The CT generates many images in a short time. A computer fuses them and generates multiplanar reconstructed images. This method permits the examination of anatomical structures in any position imaginable. However, the transversal, sagittal and coronal aspects are most commonly used. (41)

Diagnostic value of the CT in G1 and G2 gastric NETs is limited. It only detects large, invasive neoplasms. Sizable, solitary NET lesions include G3 gastric tumours.(41)

1.10.2 Magnetic Resonance Imaging

Magnetic resonance imaging (MRI) also is a multiplanar imaging tool. Unlike the CT, it does not use X-rays. The MRI shows high contrasts between neoplasms and physiological tissue. High soft tissue contrast makes detection of small NETs possible. (42) This feature poses superiorities to the CT-imaging in diagnosing tumours of the abdomen, bone, and brain. (41) However, this technology also has some disadvantages. The MRI is more expensive than the CT, has a longer scanning time, and is not accessible in all hospitals. Moreover, a longer scanning time makes patient cooperation mandatory, which plays an important role in the final image quality.(42)

1.10.3 Endoscopic procedures

Endoscopic examination of the GI-tract presents a remarkable role in detection and management of GI-NETs. It is the leading diagnostic tool for GI-NETs of unknown primary sites, despite the fact that detecting small neuroendocrine tumours is challenging. (43) The biopsy needs to be histopathologically verified to establish diagnosis of a NET. (44)

There are two different types of endoscopy. The first one is the esophago-gastro-duodenoscopy, which is used for upper gastrointestinal NETs. The second one is colonoscopy, which detects neoplasms of the colon and ileocecal valve. Therefore, it is not possible to detect the ileum and jejunum tumours by means of classical endoscopy. In the case of midgut tumours, other modalities are needed to detect and diagnose NETs precisely.(44)

1.11 OBJECTIVE OF OUR STUDY

Our observation was that ^{68}Ga-DOTA-NOC seems to accumulate in aggressive tumors of the GI-tract, causing higher SUVmax values in ^{68}Ga-DOTA-NOC PET/CT imaging. For this reason, we suggested the hypothesis that higher SUVmax values could mean higher tumor grading, and thus SUVmax could potentially be used for staging of NETs in the GI-tract and facilitate therapy of GI-NETs.

To achieve this, we set our main goal to be the determination of the correlation between SUVmax and tumor grading (G1-G3).

Our secondary goals were to determine other possible factors that could correlate with SUVmax values, including localisation of primary, age, gender and tumor markers.

Moreover, we wanted to observe if there where changes in therapy following PET/CT scans with ^{68}Ga-DOTA-NOC.

Finally, we also wanted to quantify metastases. We determined their quantity, location and SUVmax and SUVmean values. With this data, we tried to analyse the relationship between the primary tumor site and its metastases.

2 METHODS

2.1 SETTING/LOCATION

The study was conducted in the department of nuclear medicine at the Medical University of Graz.

2.2 PARTICIPANTS

We only included patients with NETs of the GI-Tract. These participants were selected if they underwent imaging with ^{68}Ga-DOTA-NOC PET/CT prior to therapy.

Further inclusion criteria were histopathologically verified lesions containing the Grading and Ki67-Index. This data was derived from the histopathological reports.

Moreover, patients with tumour markers derived from blood like Chromogranin A, Serotonin and NSE were enrolled in our study. We performed a correlation analysis between biomarker-values with SUVmax-values from primary NET sites. The aim of this analysis was to evaluate if these values are indirectly linked together by tumour activity.

Patients who underwent surgery or any kind of therapy (e.g., chemotherapy, hormone therapy, etc.) prior to our examination were excluded. The absence of verified histopathology and pancreatic lesions were also excluded from our analysis.

2.3 STUDY DESIGN, SAMPLE SIZE

Our study has an observational and retrospective design. We collected data from 265 patients from January 2015 to October 2019. With our exclusion and inclusion criteria applied, thirty-one patients have met our criteria.

2.4 PET SCANS

PET scans were performed using two different integrated PET/CT scanners (Discovery, GEHealthcare, Milwaukee, U.S.A and Biograph mCT, Siemens, Erlangen, Germany).

Initially, low-dose CT scan acquisition was performed followed by a PET scan, which was acquired from skull base to mid-thigh.

The examinations were performed 60min post injectionem and patients had to void their bladder and deposit all metallic items before examination. Informed consent had to be given by the patients for the imaging procedure. This consent was not related to our study. The dosage of ^{68}Ga-DOTA-NOC was measured dependent on the patient bodyweight. The mean dose of applied ^{68}Ga-DOTA-NOC consisted of 150.1 MBq.

The shooting mode was static, and the scan was three-dimensional. The whole examination included six bed positions. Each of them took 4 minutes and any further bed position 5

minutes. Approximately two hours were needed for this examination, including all process steps from anamnesis until image editing. The data were reconstructed using an iterative algorithm.

2.5 PET IMAGE EVALUATION

We used ^{68}Ga-DOTA-NOC PET/CT scans to evaluate patients with NETs of the GI-Tract. In the acquired images, we analysed the primary tumour site. We measured tumour size, volume, SUVmax and SUVmean. Moreover, we determined the localisation of the primary tumour. Patients presenting with metastases underwent the same analysis for each location of the metastasis.

2.6 PATIENTS HISTORY EVALUATION

Data were extracted manually from the patient data information system openMEDOCS (KAGes, Graz, Austria) ^{TM}. We retrieved patient history, including age, gender, tumour markers and therapy.

Moreover, histopathological evaluation, including grading (G1-G3), differentiation and Ki-67idex were retrieved from histopathological reports.

For data storage we used tables in Microsoft Excel 2010^{TM}. After completion of this table, we anonymized patient data using numerical encryption.

2.7 STATISTICAL TOOLS

We used the Kolmogorov-Smirnov and Shapiro-Wilk test to determine normal distribution. Mann-Whitney-U test was performed for analysis correction in our nonparametric data. Moreover, patient data was analysed using descriptive statistics.

2.8 ETHICS

This study was performed in accordance with ethical standards laid down in the 1964 Declaration of Helsinki and its later amendments and was approved by our local ethical committee. The need for informed consent was waived for this retrospective study.

3 RESULTS

We detected a total of 19 G1, 6 G2 and one G3 primary neuroendocrine neoplasms out of 31 patients with histologically verified NET lesions.

Analysis of data was performed in two stages: the first stage consisted of the quantification of primary NET site and ^{68}Ga-DOTA-NOC uptake. Distribution of age and gender was analysed. Parameters linked to clinical management of GI-NET (tumour markers, therapy modalities used following ^{68}Ga-DOTA-NOC scans) where evaluated.

In the second phase, we analysed metastases. These tests were performed to determine aggressive properties of primary NETs. Finally, we described severe metastases of a G3 NET.

3.1 PARTICIPANT CHARACTERISTICS

Table 1: Patient characteristics

PATIENT CHARACTERISTICS	**Number of patients**	**SUVmax median**	**SUVmax IQR**
SEX			
male	11	22.3	5.6-57.7
female	20	9.7	4.1-27
Stage			
localised	17	11.7	4.3-38.2
metastases	14	20.8	8.6-32.5
Treatment			
Surgery	12	34.9	5.6-45.8
Chemo therapy	3	50.5	1.8-113.7
SSA	7	50.5	32.6-57.7
PRRT[1]	2	2.3	-
Watchful Waiting[2]	15	3.76	3.8-11.7
WHO Ki67-Index 2010 (%)			
G1	19	11.7	3.8-50.5
G2	6	24.6	4.4-36
G3[1]	1	1.8	-

[1]: not enough data points available, calculation of median and IQR not possible or feasible [2]: Includes routine follow-up examinations with endoscopy and other imaging modalities

Overall, 31 patients (20 females and 11 males, mean age 65.8 ± 11.9; range: 44-88 y) with GI-NETs were included in the study. Women are prone to have higher incidence of presenting NETs. G1 NET tumours were presented in 63.2% of female patients. In G2 NET tumours the incidence was even higher in 83.3% of female patients and only 16.7% in male

patients. We did not observe any different tracer uptake patterns concerning the gender of our patients.

The female to male distribution showed 20 (64.5%) females, and 11 (35.5%) males. Gender shows no correlation with SUVmax.

For further analysis we had to exclude 5 patients, leaving us with 26 data left. The reason for the exclusion of these participants was missing data, because some patients were treated externally, and we could not access their reports or history.

3.2 RESULT MAIN OBJECTIVE

We observed correlation between age and SUVmean values ($r = .37$; $p = .042$), in a way that higher age results in a higher SUVmean. (Figure 7) Age and SUVmax values did not show a significant correlation with age. Our patient collective was aged 44 to 88 years old (65.82 mean, SD=11.86).

Correlation analysis was performed with SUVmax and SUVmean values, respectively. However, SUVmean values did not show significant correlation to other parameters, with the exception of patient age. For this reason, SUVmean values were excluded in the following parts of the result section.

SUVmax values differ depending on primary site localisation ($p = .042$) and are depicted in table 1. The large intestine and stomach show the lowest SUVmax values, the highest SUVmax value was observed in the duodenum. (Figure 8)

SUVmax has no correlation with the tumour grading G1 and G2 (calculated p-value of 0.78 derived from the Mann-Whitney-U test). The median SUVmax of all tumours was 16.5 (IQR of 4.3-38.6). G1 NETs show lower SUVmax values (median=11.7, IQR=3.8-50.5) compared to G2 neoplasms (median= 24.55, IQR=4.4-36.75).

Table 2: Primary tumour sites and their ^{68}Ga-DOTA-NOC uptake measured in SUVmax.

LOCATION	SUVmax			
	Valid N	Median	Minimum	Maximum
Ileum	2	45.4	38.2	52.6
Ileocoecal	4	44.75	22.3	57.7
Jejunum	2	27.05	21.5	32.6
Duodenum	6	16.5	5.57	141.5
Stomach	2	6.33	3.76	17.6
Colon	4	6.05	3.31	36
Coecum	2	4.78	1.76	7.8
Rectum	4	3.14	1.27	73.7

Figure 7: Scatterplot of SUVmax, SUVmean and age. SUVmean shows a significant correlation to age, whereas SUVmax does not correlate with age.

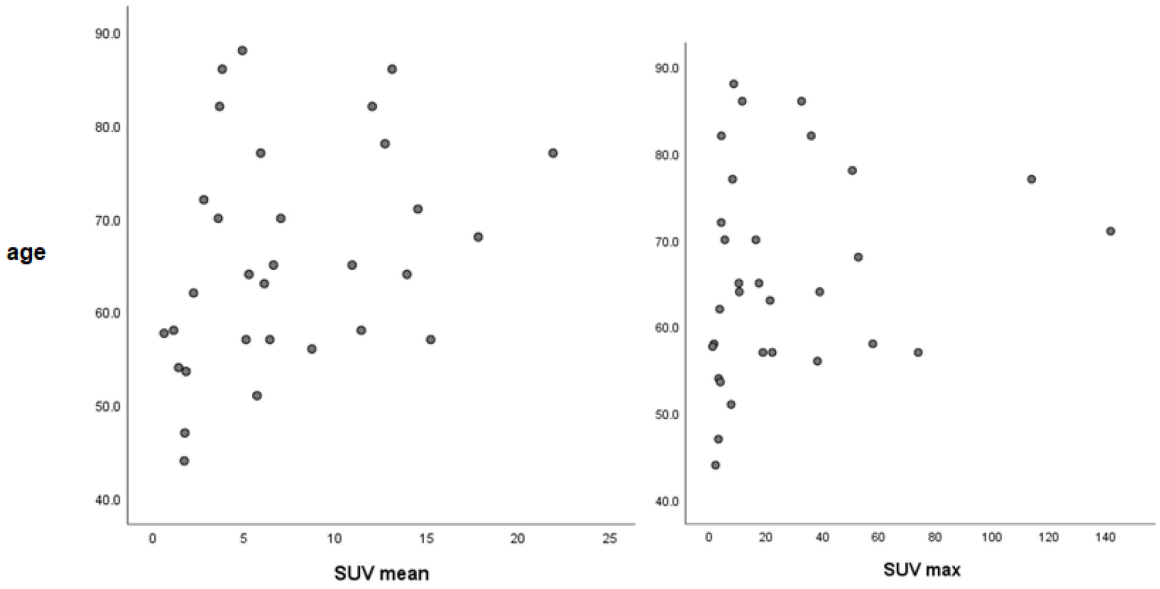

Figure 8: SUVmax and primary tumour location. High SUVmax values were observed in the duodenum. Low SUVmax values were present in gastric NETs and neoplasms of the coecum, colon and rectum.

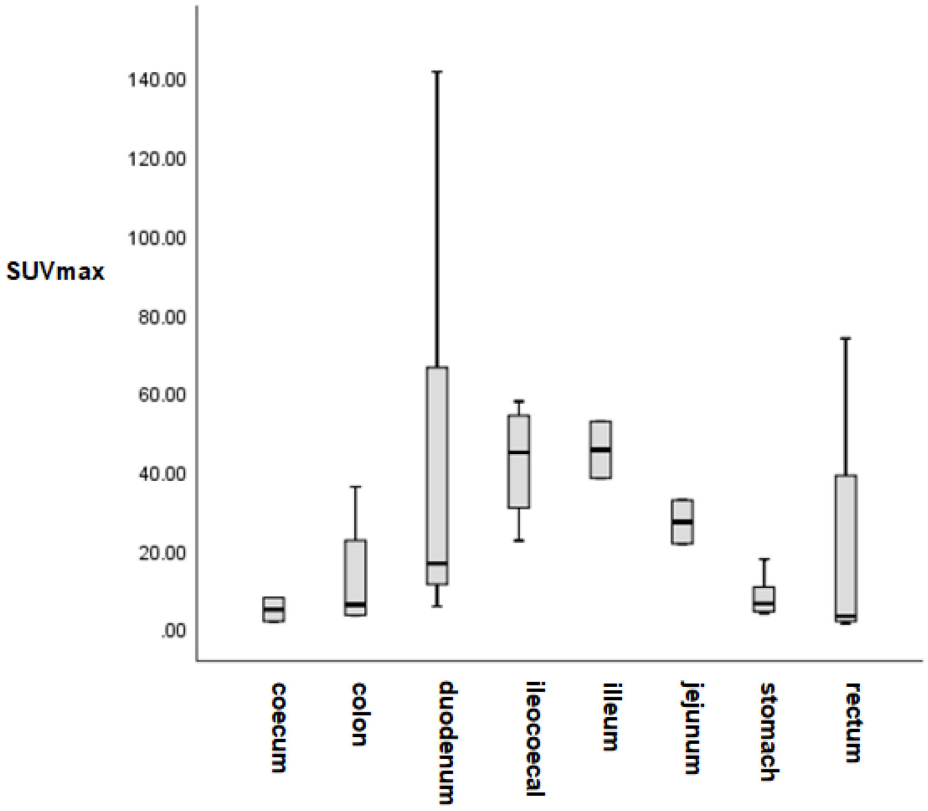

3.3 CLINICAL MANAGEMENT

3.3.1 Tumourmarkers

Chromogranin A, Serotonin and NSE did not correlate significantly with SUVmax values as depicted in table 3. However, serotonin shows a slight correlation with SUVmax values of NETs in the ileum.

Table 3: Correlation and number of tumour markers in relation to primary tumour sites.

Tumour marker	**SUVmax**					
	Stomach	Jejunum[1]	Ileum[2]	Colon[3]	Rectum	Total
Serotonin						
p	0.391	0.337	0.005	-	0.600	0.061
n	5	7	6	2	4	24
NSE[4]						
p	0.600	0.645	.493	-	0.800	0.379
n	4	7	8	2	4	25
Chromogranin A						
p	0.208	0.406	0.531	0.667	0.600	0.920
n	6	9	8	3	4	30

[1]: includes NETs in the duodenum. [2]: includes ileocoecal NETs. [3]: not enough data points available, calculation of significance not possible or feasible. [4]: Neuron-specific-enolase

3.3.2 Therapy

Watchful waiting was the main and/or the additional therapy of choice in 15 cases and correlated with lower SUVmax values. (Median= 5.57, Range 1.27-19, p=0.001) Seven patients treated with SSA had significantly higher SUVmax values (Median = 50.5, Range 21.5 - 73.7) compared to patients without SSA therapy (Median = 8.5, Range 1.27 - 141.50) (p = 0.001). Surgery was performed in twelve cases; chemotherapy was performed in three cases and radioligand therapy was initiated two times. These therapy modalities did not correlate with SUVmax.

3.4 METASTASES

Out of 31 patients with confirmed NET, 14 cases presented metastases. We detected a total of 75 lesions with suspicious ^{68}Ga-DOTA-NOC accumulation and uptake, depicted in table 2. Gastric NET did not show any metastases, whereas primary tumours in the SI commonly

express secondary tumour sites in the bone, liver and lymph nodes. Figure 9 and 11a show a 78-year-old patient with G1 NET. The primary tumour site was situated in the valvula ileocoecalis. Multiple metastases were present in the liver, lymph nodes and bone. The patient was treated with somatostatin analogs (Leotrid)® since 2018 in a palliative setting. However, the patient did not undergo surgery.

Figure 9: G1 NET with primary tumour site in the valvula ileocoecalis. A: Primary lesion. B: Secondary tumour site in the liver. C: Metastasis in the proximal femur bone. D: Metastases in the infrarenal lymph nodes.

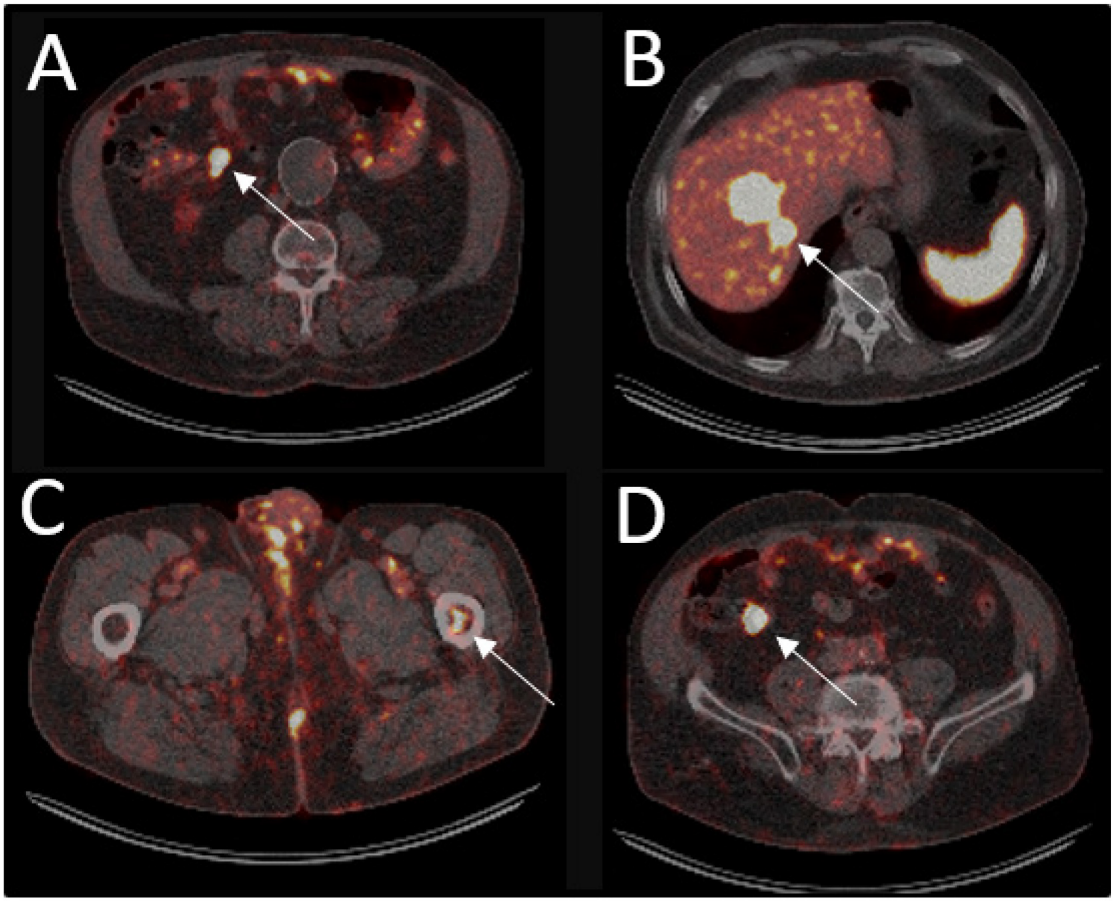

Table 4: Number and location of metastases detected with ^{68}Ga-DOTA-NOC PET/CT scans in relationship to GI-NET primary site.

PRIMARY SITE		**METASTASES**			
Location	n	Small Intestine	Bone	Liver	Lymph node
Stomach	6	-	-	-	-
Duodenum, Jejunum	9	-	5	9	2
Ileum, Ileocoecal, Coecum	8	2	5	6	7
Colon	4	-	-	-	2
Rectum	4	-	-	2	4

3.4.1 Special Case with G3

Correlation analysis of G3 NETs was left out because it was only present in one patient. However, the severe metastases of this tumour can be seen in figure 10 and 11b.

This patient presented with Neuroendocrine Carcinoma (NEC) of the coecum. This neoplasm had a KI67-Index between 80 and 90%. Furthermore, metastases were present in lymph nodes, liver, lung, bone, and the brain. The patient died two years after initial diagnosis of the neuroendocrine neoplasm. The physical examination showed signs of choledocholithiasis, with icteric changes of the sclera and the dermis. Furthermore, the patient was hospitalised because of hematemesis.

The body composition and nutrition status where severely reduced and a confused state of mind was present.

The therapeutic interventions included diagnostic probe excision of the primary tumour site. Emergency laparotomy was performed, leading to hemicolectomy and ileostomy. Metastases of the brain were treated with radiation therapy. Further interventions included Port-à-Cath-implantation, palliative chemotherapy with Cisplatin/Etoposid, watchful waiting and best supportive care.

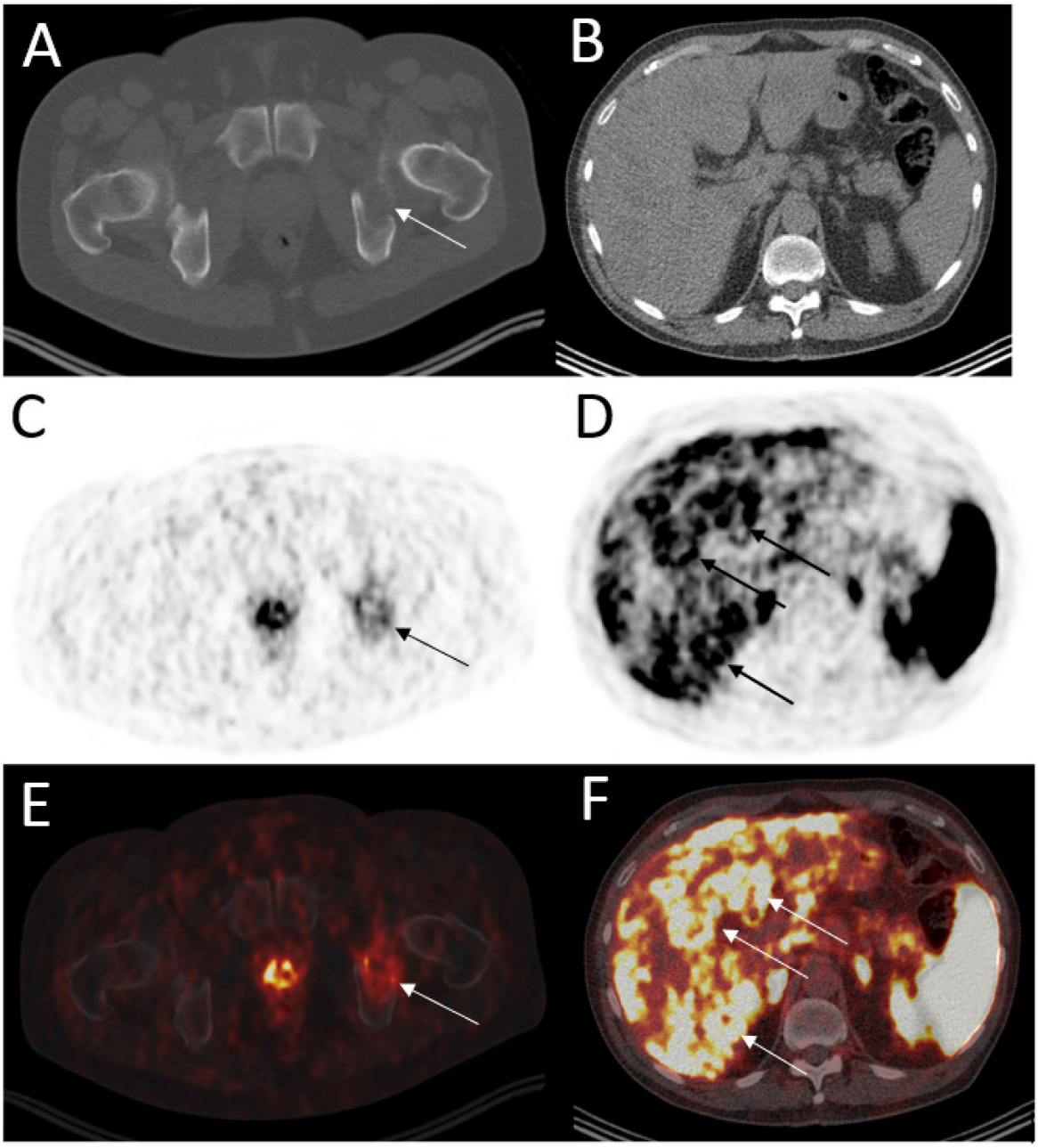

Figure 10: G3 NET metastases with colon as primary site, which was removed prior to the examination. A: CT image with bone window. The arrow indicates a secondary lesion in the hip bone (acetabulum) B: CT image of the liver. The liver imposes without destinctive lesions, contrary to D and F. C: PET image, same slice as A. The secondary tumor site in the hip bone shows tracer uptake. D: PET image, same slice as B. The arrows indicate multiple metastases with tracer uptake in the liver. E: Fusion image of the hip. The secondary lesion is visible in CT and PET imaging. F: fusion image of liver metastases. The arows indicate areas which show secondary tumor lesions. PET and CT imaging combinend can show the anatomical localisation of the metastases which where not visible in CT alone.

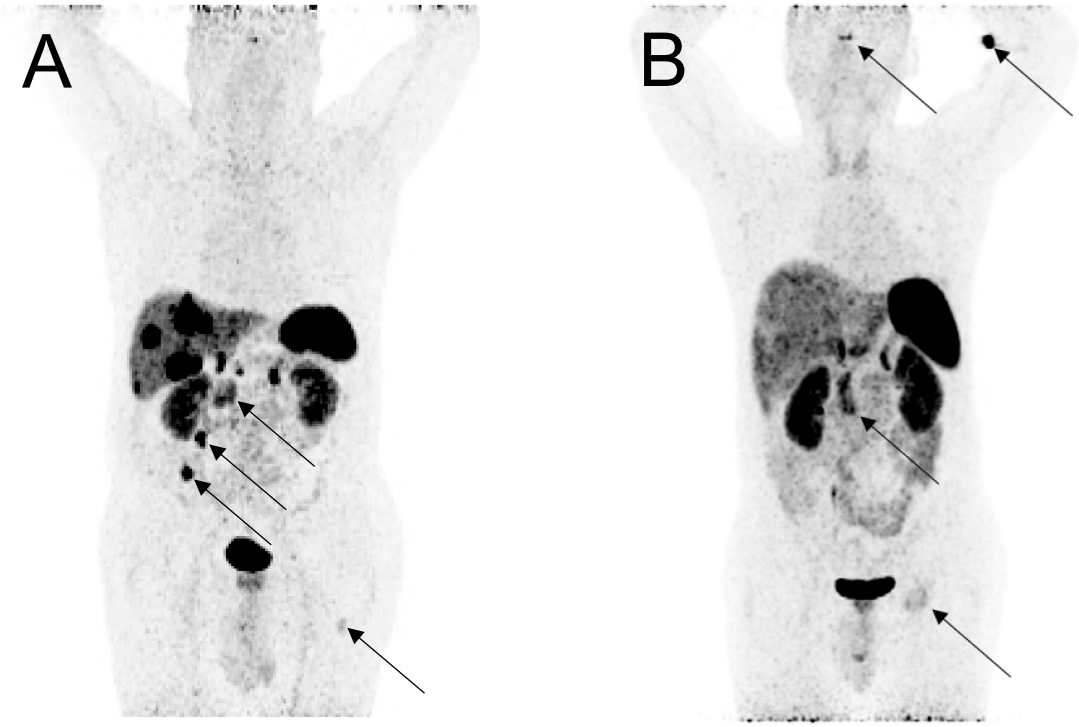

Figure 11: ^{68}Ga-DOTA-NOC PET images in coronal axis A: G1 NET, primary tumour site in the valvula ileocoecalis. Secondary tumour sites are present in the liver and the left proximal femur bone. Metastases are also present in paraaortic and infrarenal lymph nodes (right). B: G3 NET, primary tumour site in the caecum (not visible). The patient presents paraaortic lymph node metastases and bone metastasis in the acetabulum of the left hip bone. The hypophysis and Injection site are visible.

4 DISCUSSION

Females presented with GI-NET more often than men, with a female to male ratio of 1.8:1. This female predominance is similar to other studies which show a female to male ratio of 2.5:1.(4) Gender had no correlation with SUV values.

We found that age correlated significantly with SUVmean. This could mean that receptor density in GI-NETs changes with age. If this is true, age could be a factor for an indication of targeted therapies and their therapeutic outcome. We observed patients aged between 44 and 88 years, with a mean age of 65.8±11.9. The age of our patients is higher compared to findings in literature, which describe GEP-NETs occurring between 50 to 60 years of age (4). The mean age of patients presenting SI-NETs was also described lower, with a mean age of 57.9 years (range: 25-88). (45)

We found no significant correlation between SUVmax and tumour grading G1 and G2. However, SUVmax values differed significantly depending on primary tumour site.

Most of our cases presented with G1 NET. This means that GI-NETs provide enough somatostatin receptors for uptake of ^{68}Ga-DOTA-NOC for PET/CT detection. Most NETs where present in the duodenum, gaster, colon and rectum.

The jejunum, ileum and coecum were locations with lower numbers of primary NET lesions. We detected a total of six neuroendocrine neoplasms in these locations.

Our results concerning the clinical management of patients showed that SSA therapy and watchful waiting correlate significantly with SUVmax values. No correlation was found between tumour markers and SUVmax. Watchful waiting, surgery and SSA were therapy modalities of frequent use. The administration of chemotherapeutic agents and receptor therapy was used less frequently, being the therapy of choice in five cases.
Analysis of metastases showed that gastric NETs did not have metastases. Finally, we analysed our G3 NET case of the coecum. This patient presented extensive distance metastases and clinical symptoms.

Following the interpretation of our results, we decided to apply the null hypothesis. We would say that G1 and G2 do not show significant SUVmax values because the receptor

activity is similar between them. We think that this behaviour arises from the morphology of GI-NETs, which grow at a slow rate and therefore probably do not express high numbers of receptors. Moreover, the Ki67-Index used for grading is a marker for mitotic count in the nucleolus of cells and is probably not representative for receptor activity. (8) Tests between mitotic activity and receptor activity could yield no results because these activities are possibly not as strongly bound together as we thought. Moreover, Ki67-Index is evaluated under the microscope, where marked cells are counted. Cell counts between 500 and 1000 cells determine the grading. (8) This is a very meticulous process, where only a few cells can change the grading between G1 and G2. PET/CT can show different results influenced by voluntary and involuntary patient movement.(46) Involuntary peristaltic activity in the GI-tract possibly interferes with SUVmax measurement, leading to higher or lower results. Involuntary movement and resulting SUVmax deviation could be high, thereby masking a statistical correlation.

There are certain tumour markers that can indicate the presence of NETs. The most common ones are CgA, NSE, Serotonin, 5-HIAA, neurokinin A (NKA), and cluster of differentiation 56 (CD56).(12,47)
Most of our patients were tested for NSE, CgA and Serotonin. We wanted to compare the sensitivity and specificity of tumour markers with sensitivity and specificity of SUVmax. However, we realised that this test could potentially lead to selection bias. This bias could arise because we only included patients with histologically confirmed NETs prior to therapy that underwent examination with ^{68}Ga-DOTA-NOC PET/CT, and not all patients who presented themselves with a SI-NET between 2017 and 2019. For this reason, ^{68}Ga-DOTA-NOC PET/CT would always yield better results than tumour markers.

We did not detect metastases in gastric NETs. However, gastric NETs often present with low grading. Metastases are uncommon findings in these low-grade NETs.(48) Moreover, common treatment for these neoplasms is endoscopic resection and follow-up examinations. (49) ^{68}Ga-DOTA-NOC PET/CT presents a viable diagnostic tool in the detection of gastric NETs (50)(51) in addition to endoscopic procedures. We suppose that the absence of secondary tumour sites of gastric NETs in our patients is the result of early detection and resection of the primary tumour site. For this reason, our patients did not develop metastases and no secondary tumour sites are detectable with ^{68}Ga-DOTA-NOC PET/CT.

Our case presenting with G3 NET showed extensive metastases without detectable primary tumour site in ^{68}Ga-DOTA-NOC PET/CT scans. However, the primary lesion was detectable with ^{18}F-FDG PET/CT scans. This could be because ^{68}Ga-DOTA-NOC PET/CT performs better in detection of G1 and G2 NETs compared to ^{18}F-FDG imaging. However, ^{68}Ga-DOTA-NOC PET/CT is outperformed by ^{18}F-FDG scans if lesions are of higher grades, like G3 neoplasms, due to absent or diminished somatostatin receptors in dedifferentiated tumours.(52)

4.1 Assessment of study strengths and weaknesses

4.1.1 STUDY STRENGHTS

We used concise inclusive and exclusive criteria and deliberately excluded patients with therapy prior to imaging. This provides SUVmax values which are not lowered trough confounding factors of iatrogenic nature. We also included analysis of metastases, clinical factors like tumour markers and therapy in addition to our primary goal. Patients with NETs undergo treatment in a multimodal fashion(53,54), which highlights the importance of a global view of the human body.

4.1.2 LIMITATION OF TECHNOLOGY

Certain organs show physiological uptake of ^{68}Ga-DOTA-NOC. These include salivary glands, kidneys, head of pancreas, liver, and spleen. However, the spleen can form accessory spleens outside its anatomical borders. Accessory spleens are labeled physiological. (55) We had one patient with an accessory spleen. We did not evaluate this finding as a pathological lesion but documented it as a finding associated with common pitfalls.

As the name implies, PET/CT has a CT component. The radiation emerging of the CT scan should be taken into consideration in a risk-reward evaluation. However, new combined imaging modalities could bypass this problem. New diagnostic devices are in development, combining a PET scan with MRI, which lowers the overall radiation exposure and improves patient security.(33)

4.1.3 LIMITATION OF OUR STUDY

One limitation of our study was that we did not correct SUVmax with the primary lesion size. This could lead to volume effects and a wrong estimate of SUVmax. (56) (57)

Another limitation was our small cohort size. We did not have enough G3 cases to quantify them. Moreover, it would be beneficial to have similar numbers of G1 and G2 cases to test, because the results are more representative if the tested groups are similar in size.
We had to exclude four patients with gastric NETs and one patient with primary NET in the duodenum, because all of them had no significant tracer accumulation which is reconcilable with typical NET uptake patterns.
The absence of tracer accumulation in gastric NETs could be the result of endoscopic screening modalities and resection. The majority of gastric NETs have a polyp structure and are resected within gastroscopy. Most low-grade tumours are resected. (58) However, this could lead to potentially undetectable primaries in ^{68}Ga-DOTA-NOC PET/CT, because the tumour is not present anymore.

4.2 Comparison of findings with previous studies

Early detection of GI-NETs could be performed with ^{68}Ga-DOTA-NOC PET/CT, because it detects G1 and G2 tumours. These are most common stages of GI-NETs, except of oesophageal NETs, which present G3 stage in 92.1% of times. (45).

Our analyses show that there is no significant correlation between SUVmax and grading. However, it could be possible that we did not take enough factors into consideration. Campana D. et al. postulated that SUVmax can be used as prognostic factor in patients with NETs. Patients were put into two groups, depending on their Ki67 value. A cut-off value of 5% was used to differentiate between low and high-grade NETs. SUVmax was significantly higher in patients with pancreatic NET and well-differentiated NETs as well as in patients with elevated expression of SSR 2A.(35)

Our results show higher values for mean SUVmax (26.6±33.2) compared to a study which analysed neuroendocrine tumours with ^{68}Ga-DOTA-NOC PET/CT. In SI-NETs, they detected a mean SUVmax of 9.1±6.0 and 11.3±3.7 for previously unknown and known neuroendocrine neoplasms.(59) The reason for our elevated SUVmax values could be that we only included patients prior to therapy. Prasad et al. only used two inclusion criteria, histologically verified NET and unidentified primary tumour site. This means that patients possibly underwent therapy prior to PET/CT evaluation. This could lead to lower SUV values, because the tumour was already treated and shows less receptor activity.

4.3 Consideration of clinical and scientific implications

We used a cut-off Ki67-Index value of 3% and 5%. However, it seems that a standardized cut-off value for all NETs is not always the best way. Especially for ileal NETs, a cut-off value of 5% or even 1% should be used to determine between low and high-grade neoplasms. (8) We still used the standard cut off values, because they were used in the documentation of pathology. However, other cut-off values would probably yield other results and correlate with SUVmax of ^{68}Ga-DOTA-NOC PET/CT. The ideal cut-off value for Ki67-Index for SI-NETs is unknown to this day.

Most patients underwent watchful waiting, which is the result of regular endoscopic follow-up examinations. Gastric NETs were commonly linked to a watchful-waiting approach following the resection and histopathological verification of the neuroendocrine neoplasm.
In 12 cases, surgery was the treatment of choice, which could be a result of imaging and localisation of the primary with ^{68}Ga-DOTA-NOC.
Nuclear medicine modalities can change the therapeutical approach of NETs. Imaging of GEP-NETs with ^{111}In and ^{99m}Tc labeled SRS invoke a different therapeutical approach in 17 to 28% of cases.(60) This change of therapy is lower compared to PET/CT imaging with ^{68}Ga-DOTA-NOC, which brings a change in therapy in 36.5%. (33)

4.4 SUGGESTIONS FOR FUTURE RESEARCH

For future research, we suggest that more parameters should be used for staging of GI-NET with ^{68}Ga-DOTA-NOC PET/CT. In addition to SUVmax values of the primary tumour site, parameters like age, tumour diameter, prior therapy and exact location in the GI-tract should be taken into consideration. Moreover, a cut-off value of the Ki67-Index should be developed to differentiate between low- and high-grade NETs. This cut-off value should be analysed in comparison to patient outcome and therapeutic consequence.

4.5 CONCLUSION

We conclude that SUVmax values alone cannot be used to differentiate between G1 and G2 GI-NET. However, ^{68}Ga-DOTA-NOC detects lesions even in early stages of disease. Early detection of GI-NETs could provoke, or partly even trigger a change in therapy, which in turn has an impact on clinical management of these patients.

REFERENCES

1. Collins JT, Bhimji SS. Anatomy, Abdomen and Pelvis, Small Intestine. StatPearls. StatPearls Publishing; 2018.
2. Fish EM, Burns B. Physiology, Small Bowel. StatPearls. StatPearls Publishing; 2019.
3. Tirosh A, Kebebew E. The utility of 68Ga-DOTATATE positron-emission tomography/computed tomography in the diagnosis, management, follow-up and prognosis of neuroendocrine tumors. Future Oncology. 2018 Jan 1;14(2):111–22.
4. Oronsky B, Ma PC, Morgensztern D, Carter CA. Nothing But NET: A Review of Neuroendocrine Tumors and Carcinomas. Vol. 19, Neoplasia (United States). Neoplasia Press, Inc.; 2017. p. 991–1002.
5. Neychev V, Kebebew E. Management Options for Advanced Low or Intermediate Grade Gastroenteropancreatic Neuroendocrine Tumors: Review of Recent Literature. International Journal of Surgical Oncology. 2017;2017.
6. Ilett EE, Langer SW, Olsen IH, Federspiel B, Kjær A, Knigge U. Neuroendocrine carcinomas of the gastroenteropancreatic system: A comprehensive review. Vol. 5, Diagnostics. MDPI AG; 2015. p. 119–76.
7. Pathology, classification, and grading of neuroendocrine neoplasms arising in the digestive system - UpToDate [Internet]. [cited 2020 May 1]. Available from: https://www.uptodate.com/contents/pathology-classification-and-grading-of-neuroendocrine-neoplasms-arising-in-the-digestive-system
8. Klöppel G, La Rosa S. Ki67 labeling index: assessment and prognostic role in gastroenteropancreatic neuroendocrine neoplasms. Virchows Archiv. 2018.
9. Mafficini A, Scarpa A. Genetics and Epigenetics of Gastroenteropancreatic Neuroendocrine Neoplasms. Endocrine Reviews. 2019 Apr 1;40(2):506–36.
10. Ito T, Lee L, Jensenc RT. Carcinoid-syndrome: Recent advances, current status and controversies. Vol. 25, Current Opinion in Endocrinology, Diabetes and Obesity. Lippincott Williams and Wilkins; 2018. p. 22–35.
11. Cives M, Strosberg JR. Gastroenteropancreatic Neuroendocrine Tumors. CA: A Cancer Journal for Clinicians. 2018;
12. Modlin IM, Bodei L, Kidd M. Neuroendocrine tumor biomarkers: From monoanalytes to transcripts and algorithms. Best Practice & Research Clinical Endocrinology & Metabolism. 2016 Jan 1;30(1):59–77.
13. Sarrouilhe D, Clarhaut J, Defamie N, Mesnil M. Serotonin and Cancer: What Is the Link?
14. Korse CM, Buning-Kager JCGM, Linders TC, Heijboer AC, van den Broek D, Tesselaar MET, et al. A serum and platelet-rich plasma serotonin assay using liquid chromatography tandem mass spectrometry for monitoring of neuroendocrine tumor patients. Clinica Chimica Acta. 2017 Jun 1;469:130–5.
15. JÁ DP, M CF. [Chromogranin A and neuroendocrine tumors]. Endocrinologia y nutricion : organo de la Sociedad Espanola de Endocrinologia y Nutricion [Internet]. 2013 Aug [cited 2021 Oct 2];60(7):386–95. Available from: https://pubmed-1ncbi-1nlm-1nih-1gov-10013b5pe0060.han.medunigraz.at/23271036/
16. SK M, A C. Chromogranin A and its fragments in cardiovascular, immunometabolic, and cancer regulation. Annals of the New York Academy of Sciences [Internet]. 2019 [cited 2021 Oct 3];1455(1):34–58. Available from: https://pubmed-1ncbi-1nlm-1nih-1gov-10013b5pe0194.han.medunigraz.at/31588572/
17. Isgrò MA, Bottoni P, Scatena R. Neuron-Specific Enolase as a Biomarker: Biochemical and Clinical Aspects. Advances in Experimental Medicine and Biology

[Internet]. 2015 [cited 2021 Oct 2];867:125–43. Available from: https://link.springer.com/chapter/10.1007/978-94-017-7215-0_9
18. Somatostatin | C76H104N18O19S2 - PubChem [Internet]. [cited 2021 Mar 22]. Available from: https://pubchem.ncbi.nlm.nih.gov/compound/16129706#section=2D-Structure
19. Rai U, Thrimawithana TR, Valery C, Young SA. Therapeutic uses of somatostatin and its analogues: Current view and potential applications. Pharmacology and Therapeutics. 2015.
20. Barnett P. Somatostatin and somatostatin receptor physiology. Vol. 20, Endocrine. Springer; 2003. p. 255–64.
21. Zandee WT, de Herder WW. The Evolution of Neuroendocrine Tumor Treatment Reflected by ENETS Guidelines. Neuroendocrinology. 2018 May 1;106(4):357–65.
22. Herrera-Martínez AD, Hofland J, Hofland LJ, Brabander T, Eskens FALM, Gálvez Moreno MA, et al. Targeted Systemic Treatment of Neuroendocrine Tumors: Current Options and Future Perspectives. Vol. 79, Drugs. Springer International Publishing; 2019. p. 21–42.
23. Garske-Román U, Sandström M, Fröss Baron K, Lundin L, Hellman P, Welin S, et al. Prospective observational study of 177Lu-DOTA-octreotate therapy in 200 patients with advanced metastasized neuroendocrine tumours (NETs): feasibility and impact of a dosimetry-guided study protocol on outcome and toxicity. European Journal of Nuclear Medicine and Molecular Imaging. 2018 Jun 1;45(6):970–88.
24. puchem.ncbi.nlm.nih.gov, 68Ga-DOTA-NOC,2015 [Internet]. [cited 2021 Mar 21]. Available from: https://pubchem.ncbi.nlm.nih.gov/substance/58086676
25. Di Pierro D, Rizzello A, Cicoria G, Lodi F, Marengo M, Pancaldi D, et al. Radiolabelling, quality control and radiochemical purity assessment of the Octreotide analogue 68Ga DOTA NOC. Applied Radiation and Isotopes. 2008 Aug;66(8):1091–6.
26. Berzaczy D, Giraudo C, Haug AR, Raderer M, Senn D, Karanikas G, et al. Whole-body 68Ga-DOTANOC PET/MRI versus 68Ga-DOTANOC PET/CT in patients with neuroendocrine tumors: A prospective study in 28 patients. Clinical Nuclear Medicine. 2017 Sep 1;42(9):669–74.
27. Kagna O, Pirmisashvili N, Tshori S, Freedman N, Israel O, Krausz Y. Neuroendocrine tumor imaging with 68Ga-DOTA-NOC: physiologic and benign variants. American Journal of Roentgenology. 2014 Dec 1;203(6):1317–23.
28. Tetraxetan | C16H28N4O8 - PubChem [Internet]. [cited 2021 Mar 22]. Available from: https://pubchem.ncbi.nlm.nih.gov/compound/121841#section=2D-Structure
29. Soto-Montenegro ML, Peña-Zalbidea S, Mateos-Pérez JM, Oteo M, Romero E, Morcillo MÁ, et al. Meningiomas: A comparative study of 68Ga-DOTATOC, 68Ga-DOTANOC and 68Ga-DOTATATE for molecular imaging in mice. PLoS ONE. 2014 Nov 1;9(11).
30. Amor-Coarasa A, Schoendorf M, Meckel M, Vallabhajosula S, Babich JW. Comprehensive quality control of the ITG 68Ge/68Ga generator and synthesis of 68Ga-DOTATOC and 68Ga-PSMA-HBED-CC for clinical imaging. Journal of Nuclear Medicine. 2016 Sep 1;57(9):1402–5.
31. Blom E, Koziorowski J. 68Ga-Autoclabeling of DOTA-TATE and DOTA-NOC. Applied Radiation and Isotopes. 2012 Jun 1;70(6):980–3.
32. Townsend D. Physical Principles and Technology of Clinical PET Imaging †. Vol. 33. 2004.
33. Mawlawi O, Townsend DW. Multimodality imaging: An update on PET/CT technology. Vol. 36, European Journal of Nuclear Medicine and Molecular Imaging. Eur J Nucl Med Mol Imaging; 2009. p. 15–29.

34. Schöder H, Erdi YE, Larson SM, Yeung HWD. PET/CT: A new imaging technology in nuclear medicine. Vol. 30, European Journal of Nuclear Medicine and Molecular Imaging. Springer; 2003. p. 1419–37.
35. Campana D, Ambrosini V, Pezzilli R, Fanti S, Labate AMM, Santini D, et al. Standardized uptake values of68Ga-DOTANOC PET: A promising prognostic tool in neuroendocrine tumors. Journal of Nuclear Medicine. 2010 Mar;51(3):353–9.
36. Deppen SA, Blume J, Bobbey AJ, Shah C, Graham MM, Lee P, et al. 68Ga-DOTATATE compared with 111In-DTPA-octreotide and conventional imaging for pulmonary and gastroenteropancreatic neuroendocrine tumors: A systematic review and meta-analysis. Journal of Nuclear Medicine. 2016 Jun 1;57(6):872–8.
37. Decristoforo C, Melendez-Alafort L, Sosabowski JK, Mather SJ. 99mTc-HYNIC-[Tyr3]-octreotide for imaging somatostatin-receptor- positive tumors: Preclinical evaluation and comparison with 111In- octreotide. Journal of Nuclear Medicine. 2000 Jun;41(6):1114–9.
38. Hutton BF. The origins of SPECT and SPECT/CT. Vol. 41, European Journal of Nuclear Medicine and Molecular Imaging. Springer Verlag; 2014. p. 3–16.
39. Tolomeo A, Lopopolo G, Dimiccoli V, Perioli L, Modoni S, Scilimati A. Impact of 68Ga-DOTATOC PET/CT in comparison to 111In-Octreotide SPECT/CT in management of neuro-endocrine tumors. Medicine. 2020 Feb;99(7):e19162.
40. De Camargo Etchebehere ECS, De Oliveira Santos A, Gumz B, Vicente A, Hoff PG, Corradi G, et al. 68Ga-DOTATATE PET/CT, 99mTc-HYNIC-octreotide SPECT/CT, and whole-body MR imaging in detection of neuroendocrine tumors: A prospective trial. Journal of Nuclear Medicine. 2014 Oct 1;55(10):1598–604.
41. Sundin A, Arnold R, Baudin E, Cwikla JB, Eriksson B, Fanti S, et al. ENETS Consensus Guidelines for the Standards of Care in Neuroendocrine Tumors: Radiological, Nuclear Medicine and Hybrid Imaging. In: Neuroendocrinology. S. Karger AG; 2017. p. 212–44.
42. Grimaldi F, Fazio N, Attanasio R, Frasoldati A, Papini E, Angelini F, et al. Italian Association of Clinical Endocrinologists (AME) position statement: A stepwise clinical approach to the diagnosis of gastroenteropancreatic neuroendocrine neoplasms. Vol. 37, Journal of Endocrinological Investigation. Springer International Publishing; 2014. p. 875–909.
43. Attili F, Capurso G, Vanella G, Fuccio L, Fave GD, Costamagna G, et al. Diagnostic and therapeutic role of endoscopy in gastroenteropancreatic neuroendocrine neoplasms. Vol. 46, Digestive and Liver Disease. 2014. p. 9–17.
44. Yazici C, Boulay BR. Evolving role of the endoscopist in management of gastrointestinal neuroendocrine tumors. Vol. 23, World Journal of Gastroenterology. Baishideng Publishing Group Co., Limited; 2017. p. 4847–55.
45. Estrozi B, Bacchi CE. Neuroendocrine tumors involving the gastroenteropancreatic tract: A clinicopathological evaluation of 773 cases. Clinics. 2011;66(10):1671–5.
46. Mawlawi O, Townsend DW. Multimodality imaging: An update on PET/CT technology. Vol. 36, European Journal of Nuclear Medicine and Molecular Imaging. Eur J Nucl Med Mol Imaging; 2009. p. 15–29.
47. Cives M, Strosberg JR. Gastroenteropancreatic Neuroendocrine Tumors. CA: A Cancer Journal for Clinicians. 2018 Nov 1;68(6):471–87.
48. Klöppel G, Clemens A. The biological relevance of gastric neuroendocrine tumors. The Yale Journal of Biology and Medicine. 1996;69(1):69.
49. Schindl M, Kaserer K, Niederle B. Treatment of gastric neuroendocrine tumors: The necessity of a type-adapted treatment. Archives of Surgery. 2001 Jan 1;136(1):49–54.

50. Kjaer A, Knigge U. Use of radioactive substances in diagnosis and treatment of neuroendocrine tumors. Scandinavian Journal of Gastroenterology. 2015 Jun 1;50(6):740–7.
51. Sato Y, Hashimoto S, Mizuno KI, Takeuchi M, Terai S. Management of gastric and duodenal neuroendocrine tumors. Vol. 22, World Journal of Gastroenterology. Baishideng Publishing Group Co., Limited; 2016. p. 6817–28.
52. Evangelista L, Ravelli I, Bignotto A, Cecchin D, Zucchetta P. Ga-68 DOTA-peptides and F-18 FDG PET/CT in patients with neuroendocrine tumor: A review. Vol. 67, Clinical Imaging. Elsevier Inc.; 2020. p. 113–6.
53. De Mestier L, Dromain C, D'Assignies G, Scoazec JY, Lassau N, Lebtahi R, et al. Evaluating digestive neuroendocrine tumor progression and therapeutic responses in the era of targeted therapies: State of the art. Vol. 21, Endocrine-Related Cancer. BioScientifica Ltd.; 2014. p. R105–20.
54. Kulke MH, Siu LL, Tepper JE, Fisher G, Jaffe D, Haller DG, et al. Future directions in the treatment of neuroendocrine tumors: Consensus report of the National Cancer Institute Neuroendocrine Tumor Clinical Trials Planning Meeting. In: Journal of Clinical Oncology. J Clin Oncol; 2011. p. 934–43.
55. Bozkurt MF, Virgolini I, Balogova S, Beheshti M, Rubello D, Decristoforo C, et al. Guideline for PET/CT imaging of neuroendocrine neoplasms with 68Ga-DOTA-conjugated somatostatin receptor targeting peptides and 18F–DOPA. European Journal of Nuclear Medicine and Molecular Imaging. 2017 Aug 1;44(9):1588–601.
56. Prasad V, Ambrosini V, Hommann M, Hoersch D, Fanti S, Baum RP. Detection of unknown primary neuroendocrine tumours (CUP-NET) using 68Ga-DOTA-NOC receptor PET/CT. European Journal of Nuclear Medicine and Molecular Imaging. 2010 Jan;37(1):67–77.
57. Soret M, Bacharach SL, Buvat I. Partial-volume effect in PET tumor imaging. Vol. 48, Journal of Nuclear Medicine. Society of Nuclear Medicine; 2007. p. 932–45.
58. Gluckman CR, Metz DC. Gastric Neuroendocrine Tumors (Carcinoids). Vol. 21, Current Gastroenterology Reports. Current Medicine Group LLC 1; 2019. p. 1–7.
59. Prasad V, Ambrosini V, Hommann M, Hoersch D, Fanti S, Baum RP. Detection of unknown primary neuroendocrine tumours (CUP-NET) using 68Ga-DOTA-NOC receptor PET/CT. European Journal of Nuclear Medicine and Molecular Imaging. 2010 Jan;37(1):67–77.
60. Rufini V, Calcagni ML, Baum RP. Imaging of Neuroendocrine Tumors. Seminars in Nuclear Medicine. 2006 Jul 1;36(3):228–47.